

This is an electronic reprint of the original article. This reprint may differ from the original in pagination and typographic detail.

A new perspective on vegetable oil epoxidation modeling: reaction and mass transfer in a liquid-liquid-solid system

Salmi, Tapio; Russo, Vincenzo; Freites, Adriana; Tolvanen, Pasi; Wärnå, Johan; Di Serio, Martino; Tesser, Riccardo; Cogliano, Tommaso; Leveneur, Sébastien; Eränen, Kari

Published in:
AIChE Journal

DOI:
[10.1002/aic.17626](https://doi.org/10.1002/aic.17626)

Published: 01/05/2022

Document Version
Accepted author manuscript

Document License
Unknown

[Link to publication](#)

Please cite the original version:

Salmi, T., Russo, V., Freites, A., Tolvanen, P., Wärnå, J., Di Serio, M., Tesser, R., Cogliano, T., Leveneur, S., & Eränen, K. (2022). A new perspective on vegetable oil epoxidation modeling: reaction and mass transfer in a liquid-liquid-solid system. *AIChE Journal*, 68(5), Article e17626. <https://doi.org/10.1002/aic.17626>

General rights

Copyright and moral rights for the publications made accessible in the public portal are retained by the authors and/or other copyright owners and it is a condition of accessing publications that users recognise and abide by the legal requirements associated with these rights.

Take down policy

If you believe that this document breaches copyright please contact us providing details, and we will remove access to the work immediately and investigate your claim.

A new perspective on vegetable oil epoxidation modeling: reaction and mass transfer in a liquid-liquid-solid system

Tapio Salmi^a, Vincenzo Russo^{b*}, Adriana Freites Aguilera^a, Pasi Tolvanen^a, Johan Wärnå^a,
Martino Di Serio^b, Riccardo Tesser^b, Tommaso Cogliano^b, Sébastien Leveneur^c, Kari Eränen^a

a Laboratory of Industrial Chemistry & Reaction Engineering, Johan Gadolin Process

Chemistry Centre, Åbo Akademi University, FI-20500 Åbo-Turku, Finland

b Chemical Sciences Department, Università di Napoli "Federico II", IT-80126 Napoli, Italy

c Laboratoire de Sécurité des Procédés Chimiques, Institut National des Sciences Appliquées
de Rouen, FR-76800 Saint-Étienne-du-Rouvray, France

* Corresponding author's email : v.russo@unina.it

Abstract

A rigorous mathematical model was developed for a complex liquid-liquid-solid system in a batch reactor. The approach is general but well applicable for the indirect epoxidation of vegetable oils according to the concept of Nikolaj Prileschajew, implying in situ prepared percarboxylic acids as epoxidation agents. The model considers intra- and interfacial mass transfer effects coupled to reaction kinetics. The liquid phases were described with chemical approach (aqueous phase) and a reaction-diffusion approach (oil phase). The oil droplets were treated as rigid spheres, in which the overall reaction rate is influenced by chemical reactions and molecular diffusion. The model was tested with a generic example, where two reactions proceeded simultaneously in the aqueous and oil phases. The example (i.e., fatty acid epoxidation) illustrated the power of real multiphase model in epoxidation processes. The proposed modelling concept can be used for optimization purposes for applications, which comprise a complex water-oil-solid catalyst system.

Keywords: water-oil emulsion, solid catalyst, heterogeneous model, reaction, diffusion, mathematical model

Introduction

Epoxidized vegetable oils are used as chemical intermediates and bio-lubricants. An environmentally and ethically acceptable source of vegetable oils is tall oil, which is a side product from the Kraft pulping process. The dominating unsaturated fatty acids in tall oil are oleic acid, linoleic acid and abietic acid. The epoxidation concept of double bonds with hydrogen peroxide, originally proposed by the great chemist from Imperial Russia, N. Prileschajew is a rather complex reaction system. The chemical complexity originates from several simultaneous reactions in the multiphase system consisting of an oil phase and an aqueous phase: perhydrolysis, epoxidation and ring opening. In order to enhance the rate of the slow perhydrolysis step, a homogeneous or heterogeneous acid catalyst can be incorporated. Perhydrolysis of the reaction carrier, a carboxylic acid, such as formic or acetic acid, also takes place as a homogeneous, non-catalytic process in the aqueous bulk phase and in the liquid phase present in the pores of the solid catalyst. The main reaction path for perhydrolysis is the heterogeneously catalyzed process on the active sites present on the catalyst in the aqueous phase. The epoxidation reaction takes place in the oil phase: the percarboxylic acid reacts with the double bonds of the vegetable oil forming an oxirane ring. The reaction carrier, the short-chain carboxylic acid is regenerated, and water is released. Besides these reactions, ring-opening of oxirane takes place, which can lead to a spectrum of secondary products¹⁻⁸. The reactions and phases involved in the Prileschajew process are presented in Table 1.

The physical properties of the oil phase change dramatically during the progress of the reaction because the reaction product, the epoxide has a clearly higher viscosity than the reagent, the vegetable oil. This change affects especially the liquid-phase diffusion coefficients. Several correlations have been proposed for the estimation of liquid-phase

diffusion coefficients, but all of them predict that the liquid-phase diffusion coefficient is proportional to the fluidity, i.e., the reciprocal value of the viscosity⁹⁻¹¹. Consequently, the mass transfer rate in the oil phase is retarded.

A very important issue to be considered in all multiphase systems is the interaction between the chemical reaction and mass transfer. For rapid chemical reactions, the diffusion resistance can have a very strong impact on the overall rate of the process. A final judgement on this issue – whether the inter- and intrafacial diffusion affects the overall rate – can be done with well-known criteria published in literature, for instance with the Weisz-Prater criterion¹². For coupled multireaction systems, rigorous mathematical modelling of all the phenomena and numerical computer simulations can give the final answer on the interplay of kinetic and mass transfer effects. In the present system under consideration, the mass transfer resistance can principally appear inside the pores of the solid catalyst in the aqueous phase, in the stagnant liquid film surrounding the catalyst particle, inside the oil droplets as well as in the aqueous film surrounding the oil droplets. The mass transfer and kinetic phenomena are schematically illustrated in Figure 1, which assumes that the aqueous phase is the continuous phase while the oil phase is the discontinuous one. This hypothesis corresponds to the reality, because the reaction is usually carried out in the presence of an excess of the aqueous phase.

The endeavor of the current work is to develop a credible and rigorous mathematical model for a multiphase system explained in Table 1, taking all the effects previously mentioned into account. The main point of novelty of this modeling approach, compared with previous publications¹⁻⁸, is the inclusion of all the possible mass-transfer diffusion steps, both in the solid phase (i.e. catalyst particle) and oil droplets. In general, by including both terms, it is possible to fully govern the system, allowing a correct interpretation of kinetic data with the

pursuit of revealing the intrinsic kinetics of epoxidation. The inclusion of mass transfer phenomena within the oil phase is a clear novelty, as no articles which have been published take into consideration this aspect, at least for this peculiar water-oil system. The potential and the application of the new model will be illustrated by extensive numerical simulations.

Mathematical modelling of the liquid-liquid-solid reaction system

Main hypotheses of the mathematical model

The main hypotheses used in the development of the mathematical model are discussed here. The reactions are assumed to proceed in an isothermal stirred batch reactor, which operates under atmospheric pressure. A multiphase system is considered as displayed in Figure 1. The system consists of an aqueous phase, a solid catalyst phase and an oil phase. The aqueous phase is the continuous one, and oil droplets are dispersed in the aqueous environment. Chemical reactions are presumed to proceed in the aqueous bulk phase, in the pores of the solid catalyst, on the surface sites of the catalyst and in the oil droplets. No ring opening reactions were considered, as they depend on the chosen catalyst. The inclusion of this group of reactions can be responsible for the decrease of the epoxide product selectivity, a key issue that from the modelling viewpoint does not represent a problem. Thus, it is fully possible to include in this model the appropriate ring opening reaction rates, depending on the specific mechanism.

The reaction rates in the films surrounding the catalyst particles and the oil droplets are assumed to be negligible; thus, the films can be described with diffusion transport only. The governing mechanism in the porous catalyst particles and in the oil droplets is the coupled reaction-diffusion process. The oil droplets are regarded as rigid spheres, but the droplet diameter can change because of chemical reactions and the change of physical properties, i.e. mainly due to the increase of the liquid viscosity during the progress of the chemical reactions. The physical properties of the aqueous and oil phases are calculated accordingly, considering the change in the physical properties, as the reactions proceed, because changes in the liquid density and viscosity as well as the liquid-phase diffusion coefficients are expected. The change in density of the organic phase clearly modifies the volume ratio of

the two liquid phases, which has an influence on the liquid-liquid mass transfer phenomena. Thus, when interpreting real systems, this aspect must be taken into consideration.

The mean transport pore model (MTPM), also called parallel pore model^{13,14} is used for the estimation of the effective diffusion coefficients of the components present in the porous catalyst particles. Equal catalyst particle sizes and oil droplet sizes are presumed, but the model can easily be extended to comprise particle and droplet size distributions. The amount of substance adsorbed on the active sites of the catalyst is assumed to be negligible compared to the amount of substance in the catalyst pores and in the aqueous bulk phase. The model has been written in a transient form to account for the time-dependent behaviors of the component concentrations in the aqueous bulk phase, inside the catalyst pores, inside the oil droplets and on the oil droplet surface. The average concentrations in the oil phase can be easily obtained by the integration of the concentration profiles from the center to the surface of the oil droplet.

Reaction and diffusion in porous catalyst particles - Intraparticle phase

The reaction and diffusion process is illustrated in Figure 1. Both catalytic (r_c) and non-catalytic (r_{nc}) reactions proceed simultaneously inside the catalyst pores which implies that the form of the component mass balances in a volume element of a catalyst particle can be written as

$$(N_i A)_{in} + r_{ic} \Delta m_c + r_{inc} \Delta V_{Pore} = (N_i A)_{out} + \frac{dn_i}{dt} \quad (1)$$

The symbols are defined in Notation. The mass element of the catalyst is Δm_{cat} and the volume element of the pore is $\Delta V_{Pore} = \epsilon_P \Delta V$, where ϵ_P is the catalyst porosity and ΔV is the total volume element expressed as $4\pi r^2 \Delta r$ for a spherical particle. The amount of substance

in the volume element is n_i . After incorporating these definitions in equation (1) and letting the volume element to shrink ($\Delta r \rightarrow 0$), the differential equation

$$\frac{dc_i}{dt} = -\varepsilon_p^{-1} \left(\frac{d(N_i r^2)}{r^2 dr} + r_{ic} \rho_p \right) + r_{inc} \quad (2)$$

is obtained. Various approaches exist for the mathematical formulation of the diffusion flux (N_i), from the complete set of Stefan-Maxwell equations to simplified modifications based on the law of Fick (Fott and Schneider 1984). For the sake of simplicity, the mean transport pore model is applied here. It implies that individual molecular diffusion coefficients can be used, along with the correction for the porosity (ε_p) and the labyrinth structure of the pores, i.e. the particle tortuosity (τ_p): $D_{ei} = (\varepsilon_p / \tau_p) D_i$. Thus the diffusion flux of an arbitrary component (i) is expressed by

$$N_i = -D_{ei} \frac{dc_i}{dr} \quad (3)$$

After inserting this expression for the flux and the effective diffusion coefficient, and carrying out the differentiation of the flux (N_i) in equation (2), the operative form of the balance equation is obtained for a spherical catalyst particle with the radius R_p ($x=r/R_p$),

$$\frac{dc_i}{dt} = (D_{ei} / (\varepsilon_p R_p^2)) \left(\frac{d^2 c_i}{dx^2} + \frac{2}{x} \frac{dc_i}{dx} \right) + r_{ic} \rho_p / \varepsilon_p + r_{inc} \quad (4)$$

It can be easily shown that this balance equation can be generalized to

$$\frac{dc_i}{dt} = (D_{ei} / (\varepsilon_p R_p^2)) \left(\frac{d^2 c_i}{dx^2} + \frac{s}{x} \frac{dc_i}{dx} \right) + r_{ic} \rho_p / \varepsilon_p + r_{inc} \quad (5)$$

for an arbitrary geometry. In equation (5), the shape factor (s) has the following values: $s=0$ for a slab, $s=1$ for a long cylinder and $s=2$ for a spherical particle. For particles with defects on the outer surface, values $s>2$ can be found as discussed in a previous article¹⁵.

The boundary conditions for equations (4) and (5) are

$$\frac{dc_i}{dx} = 0 \quad (\text{particle center, } x=0) \quad (6)$$

$$\psi(D_{ei} / R_p) \frac{dc_i}{dx} = k_{Li}(c_{Li} - c_i) \quad (\text{outer surface of the particle, } x=1) \quad (7)$$

The first boundary condition (6) originates from the geometric symmetry of the catalyst particle. The latter boundary condition (7) implies that the diffusion flux into the pores at the outer surface of the particles is equal to the flux through the film surrounding the particle. In case of vigorous stirring, the mass transfer coefficients (k_{Li}) approach infinity and the concentrations c_i and c_{Li} become equal. In this limit case, the boundary condition (6) is replaced by $c_i=c_{Li}$ at $x=1$.

Reaction and diffusion in oil droplets

For a rigid oil droplet, the component mass balance can be described in a principally similar way to that of a porous catalyst particle. However, only non-catalytic reactions are assumed to take place inside the droplets. The primary form of the mass balance for an arbitrary component in the droplet can be written as

$$(N_i A)_{in} + r_i \Delta V = (N_i A)_{out} + \frac{dn_i}{dt} \quad (8)$$

By assuming a spherical surface area of the droplet ($4\pi r^2$) and a spherical volume element ($4\pi r^2 \Delta r$) and letting the volume element to shrink, the mass balance equation is transformed to

$$\frac{d(c_i r^2)}{r^2 dt} = - \frac{d(N_i r^2)}{r^2 dr} + r_{io} \quad (9)$$

After inserting the law of Fick into the balance equation, the relation

$$\frac{d(D_i (dc_i / dr) r^2)}{r^2 dr} + r_{io} = \frac{d(c_i r^2)}{r^2 dt} \quad (10)$$

Is obtained. The further treatment of the balance equation (10) depends on the changes of the physical properties. If the changes in the physical properties – density, viscosity, and diffusion coefficient – are negligible, an ultimate simplification is justified, and the balance equation becomes

$$\frac{dc_i}{dt} = D_i \left(\frac{d^2 c_i}{dr^2} + \frac{2}{r} \frac{dc_i}{dr} \right) + r_{io} \quad (11)$$

as the radius of the droplet remains constant. For a general geometry of the droplet, the balance equation becomes

$$\frac{dc_i}{dt} = D_i \left(\frac{d^2 c_i}{dr^2} + \frac{s}{r} \frac{dc_i}{dr} \right) + r_{io} \quad (12)$$

where s denotes the shape factor.

In case of changing physical properties of the oil phase during the reaction, the situation becomes much more complicated. If the density of the droplet changes, also the volume and the radius of the droplet change. Furthermore, the mass of the droplet increases because of the chemical reaction. The derivative in equation (10) is elaborated to

$$\frac{d(c_i r^2)}{dt} = \frac{dc_i}{dt} r^2 + 2c_i r \frac{dr}{dt} \quad (13)$$

A dimensionless coordinate is introduced, $x=r/R$ where R is the droplet radius. The differential equation is transformed to

$$\frac{d(D_i (dc_i / dr) r^2)}{r^2 dr} + r_{io} = \frac{dc_i}{dt} + (2c_i / r) \frac{dr}{dt} \quad (14)$$

i.e.

$$\frac{d(D_i (dc_i / dx) x^2)}{R^2 x^2 dx} + r_{io} = \frac{dc_i}{dt} + (2c_i / x) \frac{dx}{dt} \quad (15)$$

where $x \in [0,1]$.

For the further treatment, the following approximations are introduced: the diffusion coefficient (D_i) is presumed to be locally constant, even though its numerical value is updated during the calculations, as the physical properties of the droplet change during the reaction. The term dx/dt is neglected. The model equation becomes

$$\frac{dc_i}{dt} = (D_i / R^2) \left(\frac{d^2 c_i}{dx^2} + \frac{2}{x} \frac{dc_i}{dx} \right) + r_{io} \quad (16)$$

Two important issues have to be considered to advance with the modelling: calculation of the amounts (in moles) and concentrations of each component and the updating of the droplet radius.

The total moles of component i is obtained from the integral

$$n_{iTOT} = n_D \int_0^R c_i 4\pi r^2 dr \quad (17)$$

where n_D denotes the total number of droplets in the system. The dimensionless coordinate (x) is introduced giving

$$n_{iTOT} = n_D 4\pi R^3 \int_0^1 c_i x^2 dx \quad (18)$$

If the total number of droplets remains constant ($n_D = n_{0D}$), it can be calculated from the relation

$$n_D V_D = m_{0TOT} / \rho \quad (19)$$

The total initial mass is obtained from

$$m_{0TOT} = \sum n_{0j} M_j \quad (20)$$

Perfect spherical droplets are assumed, i.e. the initial droplet volume is

$$V_{0D} = (4/3)\pi R_0^3 \quad (21)$$

Combination of equations (19)-(21) gives

$$n_D = n_{0D} = \frac{3 \sum n_{0j} M_j}{4\pi R_0^3 \rho_0} \quad (22)$$

The total amount of substance can now be calculated from the simple relation

$$n_i = \frac{3 \sum n_{0j} M_j}{\rho_0} (R/R_0)^3 \int_0^1 c_i x^2 dx \quad (23)$$

However, an update of the droplet radius is needed. For a spherical droplet is valid

$$R = \left(\frac{3m_D}{4\pi\rho} \right)^{1/3} \quad (24)$$

If an ideal mixture is presumed, the volumes of different components present in the droplet are directly additive and the contributions of partial molar volumes are ignored. The update formula for the density becomes

$$1/\rho = \frac{\sum c_j M_j / \rho_j}{\sum c_j M_j} \quad (25)$$

where ρ_j denotes the density of an individual component in the mixture.

The mass of the droplet increases because of the chemical reaction, i.e. the epoxidation. The original mass of the droplet is

$$m_{0D} = \rho_0 V_{0D} = \rho_0 \left(\frac{4\pi}{3} \right) R_0^3 \quad (26)$$

The increase of the mass is proportional to the overall conversion of the oil (X_A),

$$m_D = m_{0D} + \gamma X_A \quad (27)$$

The conversion is defined by

$$X_A = 1 - n_A / n_{0A} \quad (28)$$

At complete conversion ($X_A=1$) the relation

$$m_{\infty D} = m_{0D} + \gamma \quad (29)$$

is valid. The final mass (m_{∞}) is obtained at complete conversion

$$m_{\infty D} = n_{E\infty} M_E \quad (30)$$

where $n_{E\infty}=n_{0A}$. Parameter γ becomes now

$$\gamma = m_{\infty D} - m_{0D} \quad (31)$$

The final mass $m_{\infty D}$ is given by equation (30) and the initial mass of the droplet is

$$m_{0D} = n_{0A} M_A \quad (32)$$

Finally, we obtain

$$\gamma = n_{0A} (M_E - M_A) \quad (33)$$

Because $M_E > M_A$, an increase of the droplet mass is expected.

The update of the droplet mass becomes

$$m_D = \rho_0 (4/3) \pi R_0^3 + n_{0A} (1 - n_A / n_{0A}) (M_E - M_A) / n_D \quad (34)$$

Recalling the definition of the number of droplets (n_D), equation (22), the final expression for the droplet mass becomes

$$m_D = (4/3) \pi R_0^3 \rho_0 (1 + (n_{0A} / (\sum n_{0j} M_j)) (1 - n_A / n_{0A}) (M_E - M_A)) = (4/3) \pi R^3 \rho \quad (35)$$

The dimensionless droplet radius at an arbitrary moment of time and conversion is now obtained from

$$y = R / R_0 = (\rho_0 / \rho)^{1/3} \left(1 + \frac{n_{0A}}{\sum n_{0j} M_j} (1 - n_A / n_{0A}) (M_E - M_A) \right)^{1/3} \quad (36)$$

The initial amounts (n_{0j}) in equation (36) are known and the initial concentrations in the oil phase are calculated from

$$c_{0j} = n_{0j} / V_L \quad (37)$$

where ρ_0 and m_{0L} denote the initial density and mass of the oil phase.

For the oil phase, the segregated oil droplets, the total amount of substance is obtained by integration of the weighted concentrations inside all the droplets,

$$n_{iO} = n_D 4\pi R^3 \int_0^1 c_{iO} x^2 dx \quad (38)$$

where the number of droplets (n_D) is given by equation (22). Consequently, the average concentrations of the components inside the droplets are calculated from

$$c_{iOav} = n_{iO} / V_O \quad (39)$$

In summary, the model for the varying-size droplets consists of equations (16), (23), (25) and (36). The density is calculated from equation (25), after which the radius (R) is updated from equation (36) and it is inserted in equation (16) which is solved numerically to obtain the concentration profiles inside the droplet. Analogous boundary conditions to equations (6) and (7) are applied for the oil droplets, but for components which are non-soluble in the aqueous phase, the boundary condition at the outer surface of the droplet becomes $dc_i/dr=0$. Typically, a concentration jump takes place at the oil-aqueous phase interface because the component solubility in both phases is seldom the same.

Bulk-phase mass balances

The bulk-phase mass balance of an arbitrary component in the aqueous phase can be developed as follows. The accumulation of the component in the aqueous phase is compensated by the transport to or from the catalyst pores and oil droplets. Based on this principle, the mass balance becomes

$$N_{ic}A_c + N_{iO}A_O + r_{inc}V_{aq} = \frac{dn_{iaq}}{dt} \quad (40)$$

The ratio of the aqueous phase-to-total volume is denoted by $\alpha=V_{aq}/V$, where the total volume is given by

$$V = V_{aq} + V_O + V_c \quad (41)$$

On the other hand, the corresponding surface-to-volume ratios are expressed as $A_c/V=a_c$ and $A_O/V=a_O$.

The diffusion fluxes N_{ic} and N_{iO} are obtained as the boundary conditions for the oil and aqueous phases,

$$N_{ic} = -D_{ei} \frac{dc_i}{dr} \quad \text{at } r=R_p \quad (42)$$

$$N_{iO} = -D_i \frac{dc_i}{dr} \quad \text{at } r=R \quad (43)$$

After inserting these very fundamental relations, the balance equation for component (i) in the aqueous phase becomes

$$(N_{ic}a_c + N_{iO}a_O + r_i\alpha)V = \frac{dn_{iaq}}{dt} \quad (44)$$

In the balance equations for the aqueous phase, the component generation rate represents in practice the non-catalytic perhydrolysis process. The amounts of substance in the aqueous

phase are obtained by numerical solution of the bulk-phase balance equation (44), coupled to the fluxes given by equations (42) and (43).

The initial amount of substance in the oil phase is

$$n_{iO} = c_{iO}V_O \quad (45)$$

where V_O denotes the volume of the oil phase, which is calculated from the total volume,

$$V_O = \beta V = (1 - \alpha - \delta)V \quad (46)$$

where α and δ denote the volume fractions of the aqueous and the catalyst phases, respectively. Thus the amount of the substance in the aqueous phase becomes

$$n_{iaq} = c_{iaq}\alpha V \quad (47)$$

and the mass balance equation (44) is rewritten to

$$\frac{dc_{iaq}}{dt} = (N_{ic}a_c + N_{iO}a_O) / \alpha + r_{inc} \quad (48)$$

For the oil phase, the segregated oil droplets, the total amount of substance is obtained by integration of the weighted concentrations inside the droplets,

$$n_{iO} = n_D 4\pi R^3 \int_0^1 c_{iO} x^2 dx \quad (49)$$

where the number of droplets (n_D) is given by equation (22). Consequently, the average concentrations of the components inside the droplets is calculated from

$$c_{iOav} = n_{iO} / V_O \quad (50)$$

Parameter α is defined as the ratio between the aqueous phase volume and the total volume,

$$\alpha = \rho_{BL} / \rho_L \quad (51)$$

where the liquid bulk phase density ($\rho_{BL} = m_{aq}/V$, V = total volume) is divided by the aqueous-phase density.

The surface-to-volume ratios are calculated from equations (52)-(53), where the catalyst ($\rho_B = m_c/V$) and the oil ($\rho_{B,o} = m_o/V$) bulk-phase densities are divided by the related intrinsic densities. For separately co-existing spherical particles and droplets is valid:

$$a_c = \frac{3\rho_B}{R_p\rho_p} \quad (52)$$

$$a_o = \frac{3\rho_{B,o}}{R_o\rho_o} \quad (53)$$

Mass transfer coefficients

In case of vigorous stirring, the mass transfer in the liquid films surrounding the catalyst particles and the oil droplets is rapid, thus the corresponding mass transfer coefficients in the stagnant films surrounding the catalyst particles and the oil droplets approach infinity. For the catalyst particles in the present application, epoxidation of unsaturated carboxylic acids, the particle radius can be regarded as constant, but the radii of the oil droplets might change due to the chemical reactions. In this sense, the actual system has similarities with reactive solids with a diminishing radius – a case recently treated in a recent article of our group¹⁵. An analogous concept can be applied on the oil droplets with a changing size.

A generally accepted correlation equation for mass transfer coefficients in the fluid films relates the Sherwood number (Sh) to the Reynolds (Re) and the Schmidt number (Sc) as follows¹⁶,

$$Sh = a' + b' Re^{\alpha'} Sc^{\beta'} \quad (54)$$

where $Sh = k_{Li}d/D_i$ and $Sc = \nu/D_i$ where $\nu = \mu/\rho$. For spherical particles and droplets $d=2R$ is valid. It can be theoretically shown that $\alpha'=2$, which is the limit value of Sh in the absence of turbulence. Different values for the empirical parameters b' , α' and β' are reported in literature, but $\alpha'=1/2$ and $\beta'=1/3$ are typical. Usually, the value of $b'=1...1.1$ is proposed. For vigorous stirring, $Re^{\alpha'}Sc^{\beta'} \gg 2$ and the correlation can be simplified. The Schmidt number depends exclusively on the physical properties of the system, whereas the Reynolds number is heavily affected by the stirring efficiency, i.e., the effect dissipated to the system through the agitation. Based on the turbulence theory of A. Kolmogoroff, M. Temkin¹⁷ has proposed the following expression for the Reynolds number,

$$Re = \left(\frac{\epsilon' d^4}{\nu^3} \right)^{1/3} \quad (55)$$

where ϵ' denotes the specific effect (in W/kg) dissipated to the system via stirring. After inserting equation (55) in equation (54) and recalling that $d=2R$, we obtain ($\alpha'=2$, $\alpha=1/2$, $\beta=1/3$) for k_{Li} ,

$$k_{Li} = (D_i / 2R) \left(2 + \left(\frac{\epsilon'}{\nu^3} \right)^{1/6} \left(\frac{\nu}{D_i} \right)^{1/3} (2R)^{2/3} \right) \quad (56)$$

The relation (56) is taken into account and the dimensionless radius $y=r/R_0$ is introduced. After some straightforward mathematical manipulations, the final expression for the mass transfer coefficient is obtained,

$$k_{Li} = \frac{D_i}{2R_0 y} \left(2 + \left(\frac{\epsilon' \rho}{\mu} \right)^{1/6} \left(\frac{1}{D_i} \right)^{1/3} (2R_0 y)^{2/3} \right) \quad (57)$$

where y is updated by using equation (36).

According to the classical film theory, the film thickness is related to the mass transfer and diffusion coefficients by $\delta_L=D/k_L$. By applying this relation on equation (57), the expression for the dimensionless film thickness is obtained,

$$\frac{\delta_L}{R_0} = 2y \left(2 + \left(\frac{\varepsilon' \rho}{\mu} \right)^{1/6} \left(\frac{1}{D_i} \right)^{1/3} (2R_0 y)^{2/3} \right)^{-1} \quad (58)$$

Equations (57) and (58) reveal interesting facts. In the beginning, $y=1$ and initial values for the mass transfer coefficient and the film thickness are obtained. As the radius is decreasing during this reaction, y diminishes, and the mass transfer coefficient increases, and the film becomes thinner and thinner.

For practical experimental applications, the update of $y=R/R_0$ will reveal how much the film properties will change during the chemical process. For catalyst particles, the dimensionless radius is constant, i.e., $y=1$, and only secondary changes of k_{Li} and δ_L/R_0 take place. In the case under consideration, epoxidation of fatty acids, changes of the density and viscosity of the aqueous phase are expected.

Summary of numerical procedures and implementation

From the formal viewpoint, the system consists of several elements. A model for the catalyst particles immersed in the aqueous phase (parabolic partial differential equations, a combined initial and boundary value problem), a model for the oil droplets (parabolic partial differential equation, a combined initial and boundary value problem) and a model for the aqueous bulk phase (ordinary differential equations, an initial value problem) are included.

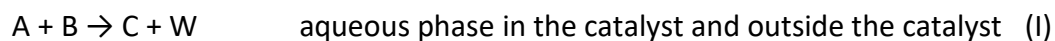
The numerical approach was based on the method of lines: the spatial coordinates of the components in the oil droplets and in the porous catalysts were discretized with central difference formulae because a diffusion problem is concerned. This operation transformed the partial differential equations (PDEs) to ordinary differential equations (ODEs, initial value problems (IVPs)) which were solved together with the ODEs describing the bulk of the aqueous phase. Second order centered finite differences, imposing 50 discretization points were used to convert the PDEs to ODEs. The entire model was implemented in the software gPROMS ModelBuilder¹⁸ (2004), which has inbuilt solvers for stiff differential equations.

Application example: from double bonds to epoxides

An application of the model developed in the previous sections is considered: a generic example demonstrating the potential and the flexibility of the model. In principle, the model is analogous with the reaction scheme of the Prileschajew process, except that the ring-opening reactions appearing in this process are neglected here.

Reaction stoichiometry and kinetics

The following simple system is considered to illustrate the potential of the model. A bimolecular reaction



is assumed to take place on the active sites of the solid catalyst (heterogeneously catalyzed process), in the pores of the catalyst (homogeneously catalyzed process) as well as in the aqueous bulk phase (homogeneously catalyzed process). The primary product (C) is soluble in the oil phase and reacts further according to the following stoichiometry



where the reactant molecule (D) is the dominating oil-phase reactant. The product (P) remains in the oil phase, while the reactant (A) mainly diffuses out from the oil phase to the aqueous phase, diffuses back into the pores of the catalyst particle and reacts according to equation (I). Molecule A is the reaction carrier (typically a short-chain carboxylic acid in the Prileschajew reaction), B is hydrogen peroxide (H_2O_2), W is water, C is the percarboxylic acid, D is the oil component (e.g. fatty acid or fatty acid ester) and P is the epoxidized product. For example, if acetic acid (A) is used as the reaction carrier, reactions I and II correspond to A +

$\text{H}_2\text{O}_2 \rightarrow \text{PA} + \text{H}_2\text{O}$ in the aqueous and the catalyst phases and $\text{PA} + \text{DB} \rightarrow \text{E} + \text{A}$ in the oil phase. A and PA denote acetic and peracetic acid, respectively and DB is the double bond in the unsaturated fatty acid.

Simple mathematical forms of the rate equations of steps I and II were used in simulations,

$$R_I = k_I c_A c_B \quad (59a)$$

$$R_{II} = k_{II} c_C c_D \quad (59b)$$

It should be noticed that the first reaction, the perhydrolysis (59a) proceeds in parallel as a catalytic and a non-catalytic process. The generation rates of the components were obtained from the stoichiometry,

$$r_i = \sum_{k=1}^S \nu_{ik} R_k \quad (60)$$

where $i=A, B, C, D, P, W$ and $k=I...II$. S is the total number of reactions ($S=2$).

Simulation results and discussion

Extensive numerical simulations were carried out to demonstrate the flexibility and versatility of the modelling approach and to investigate the effect of important material and process parameters, such as component diffusivities, catalyst particle and oil droplet radii, catalyst loading and reaction time. How to select the parameter space for simulations is always a critical issue. In this work we decided to keep the parameter space large, to reveal the behavior of the model not only under moderate but also extreme conditions.

Selection of parameters for numerical simulations

The physical properties and kinetic parameters in the numerical simulations are summarized in Table 2. The rate constants were fixed to the following values: $k_{II}=10^{-8}$, $k_{IC} \rho_P = 10^{-10}$ and $k_{INC}=10^{-12}$ (in $\text{m}^3/(\text{mol s})$) in all the simulations. It should be kept in mind that the absolute value of an individual rate parameter is not the most important issue here, as for a given kinetics the value of the diffusion coefficient de facto determines the role of the internal diffusion resistance in the process. Of course, for different values of the kinetic constants, the simulated profiles might change strongly, but the related effects could be easily explained as it is a conventional problem for consecutive reaction systems. For this reason, the attention was focused on only the investigation of the influence of the mass transfer phenomena.

The fluid-solid mass transfer resistance was considered negligible in the simulations and the mass ratio between the two phases was fixed to aqueous phase:oil= 2.5. Each phase was considered to be product-free in the beginning of the process at $t=0$. The catalyst pores were assumed to be empty of the products but filled with the reactants at $t=0$. The partition coefficient (ψ) (eq. 7) was assumed to be 1 in the simulations.

Effect of the oil-phase diffusivity

The oil-phase diffusivity can in principle vary within a wide range, because the oil-phase composition changes during the epoxidation process, the epoxidized product having a higher viscosity than the original vegetable oil. Moreover, the liquid-phase diffusion coefficient is proportional to the fluidity, i.e., the reciprocal value of the viscosity as predicted for example by the Wilke-Chang and Scheibel correlations¹⁰. The fluidity increases exponentially with temperature, as predicted by the Andrade equation¹¹, which means that the oil-phase

diffusion coefficient can vary a lot depending on the reaction temperature. Therefore, numerical simulations with different values of oil-phase diffusion coefficients were carried out.

The impact of the diffusion coefficients in the oil phase is illustrated in Figures 2-4. The numerical value of the diffusion coefficient has a profound influence on the concentration profiles inside in the oil droplet as illustrated by Figure 3, but the secondary effects, i.e. the aqueous-phase concentration profiles inside the catalyst particle are affected much less by changing the oil-phase diffusion coefficient (Figures 2, 4). This reflects the dual character of the process: the perhydrolysis process proceeds separately from the epoxidation process, in a separate phase. The concentration gradients of the original fatty acid are very flat, as expected, because the simulations were carried out by starting from pure fatty acid, which acts as a solvent in the epoxidation process.

The role of the effective diffusion coefficient in the catalyst particle

The expectations of the effect of the effective diffusion on the concentration profiles inside the catalyst particle and on the overall process are quite evident. Increasing the effective diffusion coefficients in the catalyst particle boosts the perhydrolysis, which is known to be the slow step in the Prileschajew process. With this increase of the diffusion coefficients, the overall performance can be improved as illustrated in Figures 5 and 6. According to the mean transport pore model (MTPM)¹⁴, the effective diffusion coefficient of a component depends on the molecular diffusion coefficient and the porosity-to-tortuosity ratio, which implies that by selecting a resin catalyst, a cation exchanger with a high porosity and low tortuosity could improve the efficiency of the process. However, the possibilities for a radical

improvement are limited as indicated by the simulations, which cover two orders of magnitude (from 10^{-9} to 10^{-11} m²/s for the effective diffusion coefficients).

Catalyst particle size effect

Which catalyst particle size to select is always a crucially important issue in process design. For small catalyst particles the internal diffusion resistance in the pores of the particle can be diminished, but, on the other hand, in continuous operation in packed beds, the catalyst particle size has a limit, because very small particles cause a huge pressure drop which ruins the operability. To elucidate this aspect, numerical simulations were carried out by assuming different catalyst particle sizes. Catalyst particle radii ranging from 1E-3 m to 1E-2 m were investigated. The simulation results are displayed in Figures 7 and 8. The conclusions drawn from the simulations are unequivocal: it is necessary to operate with small catalyst particles with radii less than 1E-3 m to obtain high product yields within reasonable reaction times. Luckily the commercially available ion-exchange resin catalysts have diameters 1E-3 m or less. In a previous work published by us it has been confirmed that these kind of catalyst particles are effective in practice².

Oil droplet size effect

The impact of the size of the oil droplet on the overall performance and the microcosm of the catalyst particle was studied by varying the droplet size. The simulation results displayed in Figures 9 and 10 suggest that this effect is minor. The result is strongly indicative for the practical process performance. The sizes of the oil droplets can be diminished by imposing higher and higher stirring velocities, which however increase the operation costs of the

process. The simulation results suggest that a reasonable efficiency of the epoxidation can be obtained even with rather large oil droplets.

Catalyst loading effect

Numerical simulations were carried out to illustrate the effect of catalyst loading on the rate of the process. The catalyst loading was varied in the simulations while the other parameters were kept constant. The catalyst loading was varied within a broad interval, from 33.6 to 134.3 kg/m³. A set of simulation results is presented in Figure 11. The results are very expected. By increasing the loading of the catalyst, the perhydrolysis step can be enhanced and the overall performance of the process can be improved. In the present case, the catalyst is rather inexpensive, because it is a commercial cation exchange resin (Amberlyst or Amberlite type with sulphonic acid groups), so the simulations suggest high catalyst loadings for process intensification.

Conclusions

A new mathematical model was proposed for a demanding multiphase system consisting of a continuous aqueous phase, a solid catalyst phase and a dispersed discontinuous oil phase. The model incorporated the kinetic and mass transfer phenomena in the multiphase system, both in the aqueous phase, in the oil phase and in the solid catalyst phase. The governing model equations, the mass balances were derived and solved numerically as time dependent ordinary and partial differential equations for a simplified generic multiphase system related to a real application, epoxidation of fatty acids and their derivatives. Extensive numerical studies illustrated the strong role of diffusion limitations in the catalyst particles and in the oil droplets. The new model is by no means limited to the actual case, fatty acid epoxidation, but it is generally applicable to complex multireaction liquid-liquid-solid systems coupled to complex composite kinetics of fundamental and industrial relevance. With this model, complex processes can be intensified, by selecting the optimal catalyst particle and oil droplet sizes, and in the latter case, by adjusting the stirring velocities.

Acknowledgements

This work is part of the activities financed by Academy of Finland, the Academy Professor grants 319002 (T. Salmi) and 320115 (Adriana Freites Aguilera and Pasi Tolvanen). The economic support from Academy of Finland is gratefully acknowledged.

Notation

A	surface area, m^2
a	surface area-to-volume ratio, m^2/m^3
a', b'	coefficients in the correlation for Sherwood number, -
c	concentration, mol/m^3
D	diffusion coefficient, m^2/s
d	droplet diameter ($=2R$), m
k	reaction rate constant, $m^3/(mol\ s)$
k_L	mass transfer coefficient, m/s
M	molar mass, kg/mol
m	mass, kg
N	diffusion flux, $mol/(m^2\cdot s)$
n	amount of substance, mol
R	droplet radius, m
R_p	catalyst particle radius, m
R_j	reaction rate, $mol/(m^3\ s)$ or $mol/(kg\ s)$
r_{ij}	component generation rate, $mol/(m^3\ s)$ or $mol/(kg\ s)$
r	radial coordinate, m
S	number of chemical reactions, -
s	shape factor, -
t	time, s
V	volume, m^3
X	reactant conversion, -
x	dimensionless radial coordinate, -

y dimensionless radius, -

Greek letters

α, β, δ volume ratios number in the bulk phase, -

α', β' exponents in the correlation for Sherwood number parameter in rate equation, -

γ proportionality factor, kg

δ_L film thickness, m

ε porosity, -

ε' dissipated energy, W/kg

μ dynamic viscosity, kg/(m s)

ν stoichiometric coefficient, -

ν kinematic viscosity, m²/s

ρ density, kg/m³

τ tortuosity, -

ψ partition coefficient, -

Dimensionless numbers

Re Reynolds number, -

Sc Schmidt number, -

Sh Sherwood number, -

Subscripts and superscripts

aq aqueous phase

av average

B	bulk property
c	catalyst phase, catalytic
D	droplet
e	effective
i, j	component index
k	reaction rate index
nc	non-catalytic
O, o	oil phase
L	liquid phase
P	catalyst particle
0	initial quantity

References

1. Campanella A, Baltanás MA. Degradation of the oxirane ring of epoxidized vegetable oils in a liquid–liquid–solid heterogeneous reaction system. *Chemical Engineering and Processing: Process Intensification*. 2007;46(3):210-21.
2. Freitas Aguilera A, Tolvanen P, Heredia S, González Muñoz M, Samson T, Oger A, Verove A, Eränen K, Leveneur S, Mikkola J-P, Salmi T. Epoxidation of Fatty Acids and Vegetable Oils Assisted by Microwaves Catalyzed by a Cation Exchange Resin. *Industrial & Engineering Chemistry Research*. 2018;57(11):3876-86.
3. Freitas Aguilera A, Tolvanen P, Wärnå J, Leveneur S, Salmi T. Kinetics and reactor modelling of fatty acid epoxidation in the presence of heterogeneous catalyst. *Chemical Engineering Journal*. 2019;375:121936.
4. Santacesaria E, Tesser R, Di Serio M, Turco R, Russo V, Verde D. A biphasic model describing soybean oil epoxidation with H₂O₂ in a fed-batch reactor. *Chemical Engineering Journal*. 2011;173(1):198-209.
5. Sinadinović-Fišer S, Janković M, Borota O. Epoxidation of castor oil with peracetic acid formed in situ in the presence of an ion exchange resin. *Chemical Engineering and Processing: Process Intensification*. 2012;62:106-13.
6. Tan SG, Chow W. Biobased Epoxidized Vegetable Oils and Its Greener Epoxy Blends: A Review. *Polymer-Plastics Technology and Engineering*. 2010;49:1581-90.
7. Wu ZY, Nie Y, Chen W, Wu LH, Chen P, Lu MZ, Ju F, Ji J. Mass transfer and reaction kinetics of soybean oil epoxidation in a formic acid-autocatalyzed reaction system. *Canadian Journal in Chemical Engineering*. 2016;94(8):1576-82.
8. Zheng JL, Wärnå J, Salmi T, Burel F, Taouk B, Leveneur S. Kinetic modeling strategy for an exothermic multiphase reactor system: Application to vegetable oils epoxidation using Prileschajew method. *AIChE Journal*. 2016;62(3):726-41.

9. Wilke CR, Chang P. Correlations of diffusion coefficients in dilute solutions. *AIChE Journal*. 1955;20:611-615.
10. Wild G, Charpentier JG. Diffusivité des gaz dans les liquides. *Techniques d'ingénieur*. 1987;615:1-13.
11. Reid RC, Prausnitz JM, Poling BE. *The Properties of Gases and Liquids* (4th edition). Singapore: McGraw Hill, 1988.
12. Salmi T, Mikkola J-P, Wärnå J. *Chemical Reaction Engineering and Reactor Technology* (2nd edition). Boca Raton: CRC Press Taylor & Francis Group, 2019.
13. Smith JM. *Chemical Engineering Kinetics* (3rd edition). New York: McGraw Hill, 1981.
14. Fott P, Schneider P. Multicomponent mass transport with complex reaction in a porous catalyst. In: Doraiswamy LK. *Recent Analysis of Chemically Reacting Systems*. New Delhi: Wiley Eastern, 1984.
15. Salmi T, Russo V, Carletti C, Kilpiö T, Tesser R, Murzin D, Westerlund T, Grénman H. Application of film theory on the reactions of solid particles with liquids: shrinking particles with changing liquid films, *Chemical Engineering Science*. 2017;160:161-170.
16. Wakao N. Particle-to-fluid heat/mass transfer coefficients in packed bed catalytic reactors. In: Doraiswamy LK. *Recent Analysis of Chemically Reacting Systems*. New Delhi: Wiley Eastern, 1984.
17. Temkin MI. Transfer of dissolved matter between a turbulently moving liquid and particles suspended in it. *Kinetika i Kataliz*. 1977;18:493-496.
18. gPROMS v3.7.1 User Guide, 2004, Process Systems Enterprise Ltd., London.